

**Depositional architecture and palaeoclimatic dynamics of Late Pleistocene travertines:  
Kocabaş, Denizli, SW Turkey**

EZHER TOKER\*<sup>a</sup>, MİNE SEZGÜL KAYSERİ-ÖZER<sup>b</sup>, MEHMET ÖZKUL<sup>a</sup> and SÁNDOR  
KELE<sup>c</sup>

<sup>a</sup>*Department of Geology Engineering, Pamukkale University, Kınıklı, Denizli, Turkey*

(E-mail: [egulbas@pau.edu.tr](mailto:egulbas@pau.edu.tr))

<sup>b</sup>*Department of Geology Engineering, Dokuz Eylül University, Tinaztepe, Buca, İzmir, Turkey*

<sup>c</sup>*Institute for Geological and Geochemical Research, Research Centre for Astronomy and Earth  
Sciences, Hungarian Academy of Sciences, H-1112 Budapest, Budaörsi u. 45*

**ABSTRACT**

**INTRODUCTION**

Travertines, tufas and speleothems are neotectonic, paleoenvironmental, paleohydrologic and paleoclimatologic archives of the time span that they formed (Bar-Matthews *et al.*, 1997; Hancock *et al.*, 1999; Minissale *et al.*, 2002; Andrews *et al.*, 1997; Andrews, 2006; Pedley, 2008, De Filippis *et al.*, 2012). In earlier studies, mostly tufas and speleothems have been preferred for paleoenvironmental and paleoclimatic reconstruction (Andrews, 2006; Fairchild *et al.*, 2006; Arenas *et al.*, 2010) compared to travertines (hydrothermal in origin). The main reason for this that the <sup>13</sup>C value of tufas and speleothems is influenced mostly by organic and atmospheric sources while the <sup>13</sup>C value of travertines is governed mainly by thermal sources and dissolution of primary carbonates; Horvatinčić *et al.*, 2005. However, it has been suggested that quite good results on paleoenvironmental and palaeoclimatic variations can be obtained from travertines by parallel conducting of stable isotope measurements, absolute

dating and palinological studies for a given locality. (Minissale *et al.*, 2002; Kele *et al.*, 2006, Bertini *et al.*, 2008; Uysal *et al.*, 2009).

The aim of this study is to reconstruct the palaeoenvironmental and palaeoclimatic conditions of the Late Quaternary travertines that were precipitated in a depression depositional system. For this aim, parallel investigations have been performed on depositional architecture, geochemistry, including stable carbon and oxygen isotopes, precise age determination (i.e., U/Th absolute dating method) and palynological features. As a case study, one of the travertine localities in the Denizli Basin were selected near Kocabaş settlement offering a well stratified, horizontally bedded and laterally extensive travertine body.

## **GEOLOGICAL SETTING**

The Denizli Basin, located in the Western Anatolian Extensional Province of Turkey (Fig. 1), is a graben that is bounded by normal faults along its northern and southern margins (Koçyiğit, 2005; Westaway *et al.*, 2005; Kaymakçı, 2006; Alçiçek *et al.*, 2007). The basin includes the world-famous Pamukkale travertines and many fossil counterparts (Altunel *et al.*, 1993a; Şimşek *et al.*, 2000; Özkul *et al.*, 2002; Kele *et al.*, 2011). Travertine bodies located along the northern margin of the basin (Fig. 1) were deposited at the ends of normal fault segments (e.g., step-over zones; Çakır, 1999).

The travertine deposits overlie the Neogene basin fill and older bedrocks that are exposed on the graben shoulders and in the mountainous areas. The bedrocks are mostly consisted of schists and marbles that form the Menderes Massif (Bozkurt & Oberhänsli, 2001; Erdoğan & Güngör, 2004) and the allochthonous Mesozoic limestone, dolomite, and gypsum of the Lycian Nappes, which tectonically overlay the Menderes Massif (Okay, 1989; Gündoğan *et al.*, 2008).

The Neogene fill in the Denizli Basin is formed of alluvial, fluvial and lacustrine deposits. The basin was initiated as a half graben in the late Early Miocene when deposition gradually evolved from alluvial into fluvial deposits and finally into lacustrine environments (Alçiçek *et al.*, 2007). Deposition continued until the Late Pliocene. By the Early Quaternary, there was a change in the regional tectonics and the Neogene Denizli half graben became a full graben as a result of activity along the northwest trended Pamukkale Fault zone. Quaternary deposits are evident from local fluvial terraces that become progressively younger toward to the basin center and widespread travertine deposits that are common along the northern and southern margins of the graben. The Quaternary faults and fissures that are common in the carbonate bedrocks along the margins of the graben are natural pathways that allow meteoric waters to descend into the subsurface and hydrothermal fluids to come to the surface (Minissale *et al.*, 2002; Dilsiz, 2006).

Four different travertine outcrops around Kocabaş and Gürlek areas which are named Site-I, Site- II, Site-III and Site-IV extend in altitudes ranging from 370 and 495 m asl (Fig. 1). The Site-I and Site-IV are located northern part and Site-II and Site-III of the study area (Fig. 1a &b). The studied quarries are to the southwest Highway 320 (from Denizli to Afyon). Near Kocabaş, several NW-trending inactive fissure ridges and associated bedded travertines occur (Özkul *et al.*, 2002; Altunel & Karabacak, 2005; De Filippis *et al.*, 2012). These fissure ridges have been investigated earlier from neotectonic and seismic aspects by Altunel & Hancock (1993) and they occur along the northwest margin of the basin and preferably developed at the ends of the normal fault segments or step-over zone between them. Furthermore, active and inactive outcrops of self-built channels are also commonly observed in Kocabaş (Özkul *et al.*, 2002). The formation of self-built channels is still not clarified. They can be the result of natural processes and/or man-made forms used for irrigation.

Near Gürlek, ~7 km southwest of Kocabaş (Fig. 1), the horizontally bedded travertines are exposed at ~370 m asl. The travertine benches are composed of light, medium and dark coloured horizons that are locally interbedded by palaeosols, claystone and mudstones.

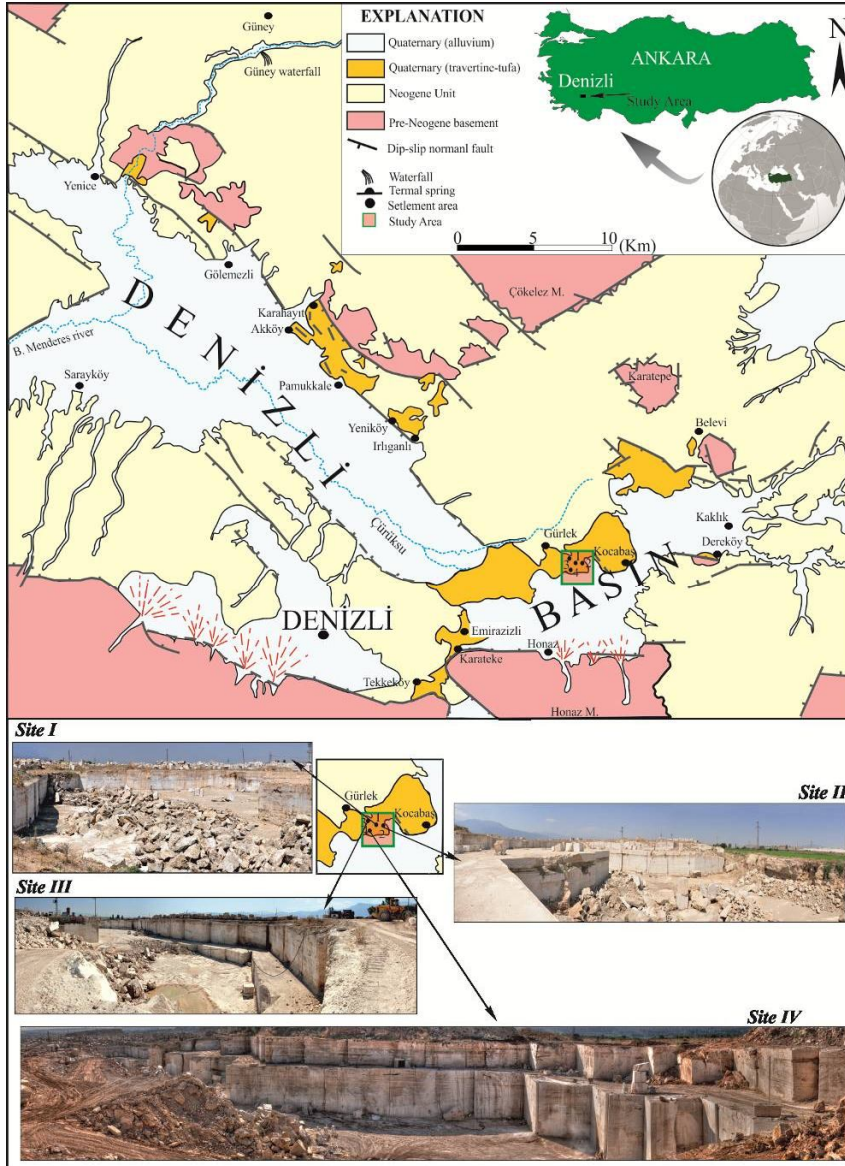


**Fig. 1** (a) Location of the Denizli area in SW-Turkey and geological map of the studied area. (b) Location of the travertine sites (Site-I, Site-II, Site-III and Site-IV) between Kocabaş and Gürlek settlements and panorama view of the main quarry

## **MATERIALS AND METHODS**

Sixty travertine samples were collected for stable carbon and oxygen isotope analyses U/Th dating and palynological investigations. During field trips besides sampling, sedimentological observations were conducted in order to determine the different travertine lithotypes and depositional systems. Geographic position and elevation of the occurrences were also determined using GPS.

### **Stable isotope analysis**

The stable isotope analyses were performed on 61 travertine samples at Institute for Geological and Geochemical Research, Hungarian Academy of Sciences, Budapest, Hungary. Carbon and oxygen isotope analyses of bulk carbonate samples were carried out using continuous flow technique (Spötl & Vennemann, 2003). Isotopic compositions are expressed in the traditional  $\delta$  notation in parts per thousand (‰) relative to V-PDB ( $\delta^{13}\text{C}$ ,  $\delta^{18}\text{O}$ ) and V-SMOW ( $\delta^{18}\text{O}$ ). Reproducibilities are better than  $\pm 0.1$  ‰ for  $\delta^{13}\text{C}$  and  $\delta^{18}\text{O}$  values of carbonates.

### **U/Th Dating**

U/Th dating was completed on 16 travertine samples at the AcmeLab (Canada). Technique is based on the precipitation of uranium at the moment carbonate deposition in the absence of thorium. After carbonate deposition, due to the radioactive decay of  $^{234}\text{U}$  the  $^{230}\text{Th}$  concentration starts increasing in the carbonate; hence the  $^{230}\text{Th}/^{234}\text{U}$  ratio of travertine depends on its age (Edwards *et al.*, 1987; Richards & Dorale, 2003).

Travertine samples were gently crushed, ultrasonicated, and dried before U/Th dating. About 50-100 mg for each subsample was selected for U/Th chemistry (Shen *et al.*, 2008) in a class-10.000 geochemical clean room with class-100 benches at the High-Precision Mass Spectrometry and Environment Change Laboratory (HISPEC), Department of Geosciences,

National Taiwan University. A triple-spike,  $^{229}\text{Th}$ - $^{233}\text{U}$ - $^{236}\text{U}$ , isotope dilution method (Shen *et al.*, 2003) was employed to correct for instrumental fractionation and determine U/Th isotopic and concentration data (Shen *et al.*, 2002). Measurements of U/Th isotopic abundances were performed on a multi-collector ICP-MS (MC-ICP-MS), Thermo Electron Neptune (Shen *et al.*, 2012). Uncertainties in the U/Th isotopic data were calculated offline (Shen *et al.*, 2002) at the level and include corrections for blanks, multiplier dark noise, abundance sensitivity, and contents of the four nuclides in spike solution.  $^{230}\text{Th}$  dates (yr BP, before 1950 AD) were calculated using decay constants of  $9.1577 \times 10^{-6} \text{ yr}^{-1}$  for  $^{230}\text{Th}$  and  $2.8263 \times 10^{-6} \text{ yr}^{-1}$  for  $^{234}\text{U}$  (Cheng *et al.*, 2000), and  $1.55125 \times 10^{-10} \text{ yr}^{-1}$  for  $^{238}\text{U}$  (Jaffey *et al.*, 1971).

### **Palynological analysis**

In the study area, palynological data were recorded from four locations. For the pollen analyses 76 samples were collected from the claystones, mudstones and travertines. The specimens were treated with HCl, HF and KOH following standard procedures (Kaiser & Asraf, 1974). The residue was sieved with a mesh-size of 10  $\mu\text{m}$ . Only twenty nine samples were found suitable for the qualitative and quantitative pollen analysis. About 150 individual palynomorphs per sample were counted. Palynomorph identification was performed under Olympus light microscope, usually at 40X and 20X magnifications. The palynomorph diagram was prepared with Tiliagraph (2.0).

## RESULTS

### Travertine lithotypes

Seven different lithotypes have been described and interpreted based on their particular features and internal structures like lamination or bedding in the measured sections. The main recognized travertine lithotypes are: 1) Laminated (L1); 2) Coated bubble (L2); 3) Reed (L3); 4) Paper-thin raft (L4); 5) Intraclasts (L5); 6) Gastropods (L6); 7) Extra-formational pebbles (L7). Paleosol bed (L8) is not travertine precipitation but it shows an erosional period when travertine deposition were probably ceased. The different travertine lithotypes in the study area are described below in detail.

*Laminated travertine (L1)*; Laminated travertine is white to light brown coloured, dense tabular deposit up to 50 cm thick overlying the reed lithotypes composed of plant clusters formed mostly longitudinal (Figs. 3&4). Lamination can be envisaged as the water runs through the quiescent pools in the supersaturated water (Pentecost, 2005) and produced by the alternation and succession of different size crystal-size laminae. Some planar voids parallel to laminations also occur and lamina thickness varies between 0.3 to 2 mm. Laminae are parallel generally with horizontal and commonly gently undulatory profiles (Fig. 3).

Generally they do not have rich organic material but in some situations, lamination is formed by alternation of micritic small shrubby cyanobacterial growths. A more laminated micritic structure is associated to algae and the continuously micro pores have been clearly observed in light coloured parallel laminated travertine levels because of microbial activity. Variations in density and colour are due to seasonal growth of the algae or bacteria. The dark colour observed in the laminated levels depends on the content of the rich Fe-Mn oxides. These horizontally bedded travertines can be interpreted as continuous laminar flows in the depression fill and this lithotype is present in all travertine sections of the study area.

*Coated bubble travertine (L2)*; Coated bubble travertine is composed mostly of coated gas bubbles and observed together with paper thin raft and reed lithotypes (Fig. 3). Carbonate-encrusted bubbles were first described by [Allen & Day \(1935\)](#) and later on by many authors (e.g. [Kitano, 1963](#), [Schreiber \*et al.\*, 1981](#), [Chafetz & Folk, 1984](#)). The term of coated bubbles is also mentioned as “lithified bubble” and “foam rock” by [Chafetz & Folk \(1984\)](#). According to [Guo & Riding \(1998\)](#) these coated gas bubbles mostly form trapped near pool surfaces below paper-thin rafts or vegetation in pools and porous sediments. In addition Guo & Riding (1998) pointed out that individual bubbles at Rapolano Terme are observed as a tube shape, aligned vertical chain, however, the shape of the bubbles in the sections is mainly spherical and oblate and their size range from millimeter to centimeter. These differences most probably related to pool width.

On the other hand thin rafts with gas bubbles imply rapid precipitation under stagnant conditions in pool environment. This lithotype is seen from at the bottom to middle part of the sections ([Fig. 4](#)).

*Reed travertine (L3)*; Reed travertine lithotype was observed as vertical and encrusted moulds of stems intercalated to coated bubbles in some part and its approximate thickness is up to 3-4 m and laterally extended a few hundred meters ([Figs.3&4](#)). These reeds are mainly obstacle to water flow, root structures stabilize the sediments and finally these plant materials encrusted by fine grained calcium carbonates which fill the space among them ([Guo & Riding, 1998](#)). Furthermore, molds of reeds, twigs, leaves and other plant structures hold on the sediments because of the obstacle to water flowing during the precipitation and mostly they were covered by micritic carbonate.

Reed, shrubs or plant materials are most probably responsible for the high porosity of the deposits and their organic matter content is much higher than in other travertine lithotypes. In



general reed, grass and other plants grow further from the orifice of hot springs where the water is cool or diluted by rain. This lithotype is generally observed mostly at the middle part of all sections (Fig. 4).

*Paper-thin rafts (L4)*; Paper-thin rafts lithotype is composed of few thin individual sheets pointed to water films and accompanied with coated bubbles and reed lithofacies (Figs. 3&4). This lithofacies is described as “paper thin raft” by Guo & Riding (1998) and formed on the floor of stagnant pools filled with still water (Guo & Riding, 1998; Özkul *et al.*, 2002). Primarily, paper-thin rafts which is also used to “hot water ice” (Alen & Day, 1935), “calcite ice” (Bargar, 1978) and “calcite rafts” (Folk *et al.*, 1985) were observed in hot spring environments as well as in cool water cave pools (Baker & Frostick, 1951; Black, 1953). Paper-thin rafts are thin, delicate, friable crystalline layers precipitated at the water surface and the crystals are preferentially horizontally oriented (e.g. Chafetz & Folk, 1984; Guo & Riding, 1998; Jones & Renaut, 2010; Özkul *et al.*, 2002). The colors of rafts range from beige to light brown, based on chemical composition of the water.

Paper-thin rafts are associated with reeds and plant materials and can be observed dominantly in the middle of all sections (Fig.4).

*Intraclast travertine (L5)*; Intraclast travertine lithotype is light brown, beige coloured totally composed of travertine fragments with different size (Fig. 3). These lithoclasts were precipitated *in situ*, particularly on the lower slope and in depressions (Guo & Riding, 1998). The size of clasts is approximately 3-4 cm, while the interclast layers are 40-50 cm thick. Furthermore, clasts are poorly sorted, angular to sub-rounded and parallel to the flow direction. The oxidation level can be observed in some parts and fragments are cemented by muddy sediments, especially where fractures are visible on the surface of the travertine body in section-II (Fig. 4). The fragments of this travertine lithotype are manifested as scour

channel fill deposits settled in the top of the parallel laminated travertine facies (Fig 3). Intraclast travertine lithotypes are clearly observed in all quarries as a key level (except Site-IV) (Fig. 4).

*Micritic travertines including gastropods (L6)*; The high proportion of small snails is a common characteristic feature of Kocabas travertine precipitation (Fig.2). The thickness of this layer included gastropods is varying in each section ranging from 40 centimeters to 2 meters. Gastropods are present at different parts of the travertine sequences indicating lake margin depositional environment. This lithotype is clearly observed at different parts of all sections as a key level (Fig.4). In figure 2 show that unidentified gastropods shells, crap fragments and leaf fossils are very common in Site-IV.



Fig. 2. General overview of travertine deposits in Site-IV and it can be clearly observed gastropods, crap fagments and leaf molds covered by  $\text{CaCO}_3$

*Extra-formational pebbly travertine lithotypes (L7)*; Pebbles are well-rounded, matrix-supported and mostly derived from ophiolitic rocks such as dunite, serpentinite and gabbro (Fig.3). In addition, these pebbles have been observed as channel-shape bodies in the travertine. The thickness of this lithotype is approximately 50 cm. These rounded pebbles with few mm in diameter in the studied travertines presumably derived from ephemeral floodings from Neogene and pre-Neogene basement rocks juxtaposed to travertine accumulation environments (Özkul *et al.*, 2002). This lithotype can be seen in the margin of the Section-II (Fig. 4).

*Palaeosol (L8)*; Palaeosols are dark brown to grey colored, rich in organic matter and the thickness of these loose continental detritus ranges from 10 to 50 cm overlying the reed lithofacies (Figs. 3 and 4). These unconsolidated materials were altered by exposure to rainwater, biological activities and subaerial desiccations associated with soil formation (Guo & Riding, 1998). With the exception of Site-III the total pollen and spore concentration was quite high in the palaeosols (Fig. 4). Each palaeosol layer constitutes a sequence boundary between two different travertine beds and this erosive surface locally enhanced by the presence of dark clays. This lithotype can be clearly observed in all sections (Fig. 4).

### **Depositional system and facies**

The depositional system in travertine precipitation describes a specific environment in which the deposition occurred and it can be delineated based on different parameters such as physical (grain size, components, erosional features, bedding), chemical (inorganic, dissolution, precipitate) and biological activities (microbial). Three main depositional systems were identified by Guo & Riding (1998), namely the Slope Depositional System, Depression Depositional System and Mound Depositional System. Chafetz & Folk (1984) named lake-fill deposits based on the morphology of the travertine accumulation.

Depositional systems can be further subdivided into facies and one facies contains several lithotypes as mentioned above in details. Guo & Riding (1998) defined the terrace slope facies, 'smooth slope facies' and waterfall facies' as a part of the Slope Depositional System. Furthermore, The Depression Depositional System is subdivided into 'Shrub flat facies (including laminated and gas bubbles)' and Marsh-pool facies (including intraclasts and reeds)' (Guo & Riding, 1998; Özkul *et. al.*, 2002). The 'Reed Mound Facies' is typical for the Mound Depositional System. Kocabaş travertines were precipitated in Depression Depositional System and it has been considered three facies as 'flat pool facies', 'shrub flat facies' and 'marsh pool facies' in this study.

#### *Flat pool facies*

Flat pool facies has been used for horizontally laminated travertine precipitations. This facies is mostly characterized by the lighter and darker lamina with a wavy transition (Fig.). This transition which means variations of colour and density in lamination are sourced by seasonal changes occurred of algal filaments. The whitish layers are generally characterized by a mainly of chemical precipitation on the other hand the darker layers correspond to the incorporation of organic components. The darker lamina is more porous than the whitish part. In general, this flat pool facies is characterized by a reed absence, parallel laminated (L1) travertine precipitation and clearly observed around 2-4 meter thickness towards to top of the all of the sections (Fig. 4). The flat pool facies is formed in shallow ponds to marshes and it is most probably like to be deposited distally from the source (Fig. 10).

#### *Shrub flat facies*

The term Shrub flat facies has been used by Guo & Riding (1998) for light coloured, thin bedded horizontal shrub travertine deposits that form units several meters in thickness and ten

to hundreds of meters in lateral extent. Shrub flat facies is composed of thin layers of shrubs intercalated with fine and crudely laminated mud layers. The shrubs are mostly micritic appearance and the spaces between shrubs are generally occupied by sparry calcite cement (Guo & Riding, 1994).

Shrubs are described by numerous authors and this term has been also used such as “micrite/spar-rhomb shrubs” by Guo & Riding, (1994), “needle crystal shrubs” by Casanova (1986) and Pentecost (1990). Shrubs are short, stubby, dense crystalline masses of CaCO<sub>3</sub> that growth upward by irregular branches (Chafetz & Folk, 1984; Guo & Riding, 1994). These branches have been occurred by algal filaments consisted of micritic fabric (Brasier, 2011; Guo & Riding, 1994). Calcitic shrubs, generally <3cm high, are characterized by an upward-expanding, irregular dendritic morphology (Chafetz & Meredith, 1983; Chafetz & Folk, 1984; Guo & Riding, 1994, 1998; Chafetz & Guidry, 1999; Jones & Renaut, 2010). This facies mostly composed of laminated (L1), reed (L3), intraclast (L5), gas bubble (L2), paper-thin raft (L4) and paleosol (L8) lithotypes (Figs.4&10). The shrub flat facies is obviously observed different parts of the whole sections and this facies mostly grow in terrace pool and depression depositional systems.



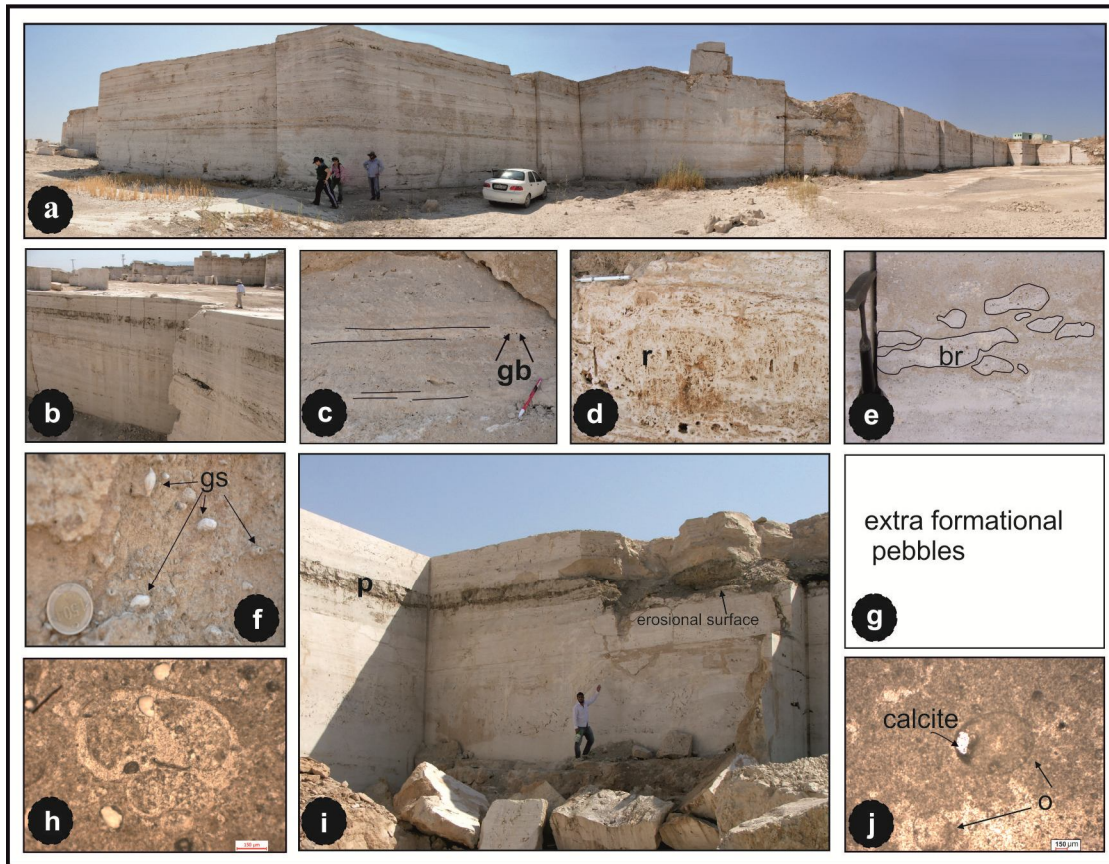
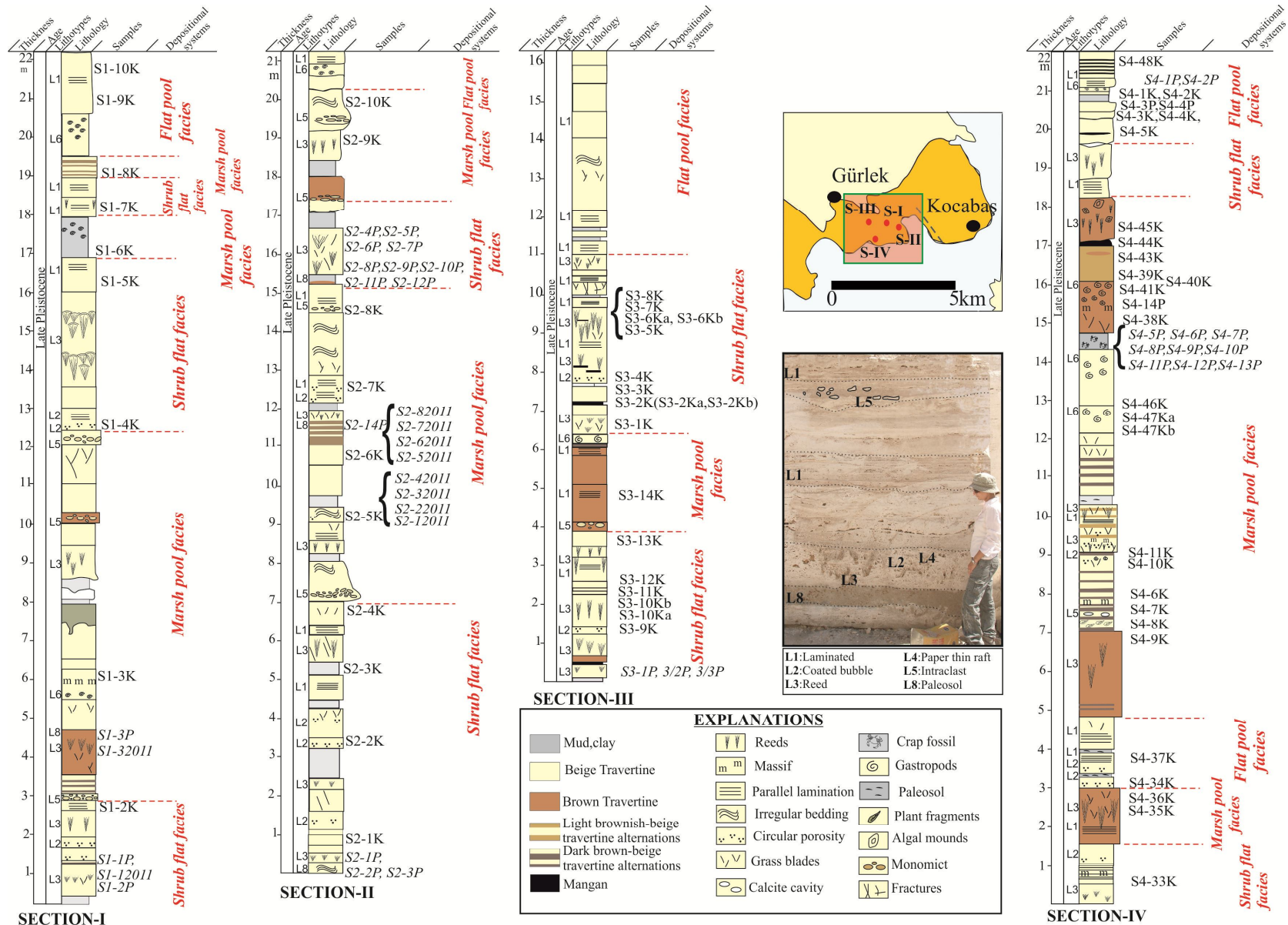


Fig. 3. a) Detail of the Depressional Depositional System in the Kocabaş area. The wide, horizontal travertine deposits formed in stagnant/low energy water are evident; b) well bedded, parallel laminated travertine, palaeosol layer is also clearly visible between travertine deposits; c) gas bubbles (gb) in flat pool facies and the horizontal lamination is accentuated (black line); d) vertical and encrusted moulds of stems (reed travertine) intercalated with gas bubbles, e) angular and subangular travertine fragments called intraclasts (travertine breccias-br) are common lithotype in marsh pool facies; f) gastropods are locally common in marsh-pool facies;(gs) are clearly visible in detritic levels of travertine deposits; g) extra formational pebbles formed sparse rounded shape are observed margin of the travertine deposits; h) microscope image, gastropod shell surrounded by micritic cement in thin section i) unconformity between two travertine precipitation highlighted by a palaeosol and intense alteration of rocks; j) Microscope image, ostracods (o) surrounded by micritic cement but inside spar calcite

### *Marsh-pool facies*

Marsh-pool facies term has been used by Guo & Riding (1998) for gray to brown lithoclast and reed travertines (L5&L3). Marsh-pool deposits are commonly interlayered with “shrub flat deposits” which are darker, brownish coloured and comprise lithoclasts (mostly hillwash breccias). In addition, gastropods, ostracodes are locally common (L6 lithotype) (Figs.3, 4&10). Pedogenic effects are locally intense (Section-IV) and these deposits form in shallow lake or pool environment where they accumulate in distal place from the source of hot spring water where water temperature is lower than in case of shrub flat deposits due to mixing with surface rainwater. Additionally, according to Guo & Riding (1998) stagnant lakes or pools fed by sulfur-rich springs display the greatest percentage of bacterially precipitated travertine (e.g. H<sub>2</sub>S-rich bath at Bagni di Tivoli). Unfortunately, we were unable to observe this kind of lake-fill travertine during their formation, however it can be obviously recognized that the depositional patterns on the quarry walls exceedingly support this interpretation.



**Fig. 4.** Illustrated correlated sections, lithotypes and depositional systems of Kocabaş travertines



## Geochemistry

### *Elemental composition*

**Table 1.** Elemental

<b>Samples</b>	<b>Ca (ppm)</b>	<b>Mg (ppm)</b>	<b>Si (ppm)</b>	<b>Fe (ppm)</b>	<b>Al (ppm)</b>	<b>Na (ppm)</b>	<b>K (ppm)</b>	<b>Ba (ppm)</b>	<b>Sr (ppm)</b>
<b>4/1K</b>	395100	2600	1300	400	0	0	0	17	857.1
<b>4/9K</b>	395800	3200	6000	400	0	0	0	9	759.6
<b>4/10K</b>	394900	3500	1300	500	200	0	0	15	929.3
<b>4/17K</b>	395000	2500	1600	800	200	0	0	17	938.3
<b>4/20K</b>	395200	2600	2100	800	300	0	0	21	932.0
<b>4/23K</b>	395000	2500	1100	500	100	0	0	14	963.0
<b>4/35K</b>	388100	3200	5600	1500	1200	100	200	29	762.0
<b>4/37K</b>	387800	3600	5700	1800	1700	0	300	28	878.9
<b>4/40K</b>	391100	4300	2300	1000	400	100	100	28	1290
<b>4/44K</b>	390100	4600	3700	500	600	0	0	28	1296
<b>3/2K(b)</b>	394400	4600	700	400	0	100	0	16	1156
<b>3/4K</b>	394100	3700	900	400	100	100	0	18	940.0
<b>3/5K</b>	396500	2900	700	500	0	0	0	19	784.5
<b>3/6K(a)</b>	395200	3200	500	400	0	0	0	11	873.9
<b>3/11K</b>	396000	2000	1000	600	200	0	0	13	739.5
<b>3/13K</b>	398600	2300	600	400		0	0	9	642.3

**I HAVE ADDED Sr VALUES ON THE TABLE**

The Sr content measured from Site-III and Site-IV in Kocabaş area displays a range: 642 – 1296ppm (Table 1).

## Isotopic Composition and Dating

### *$\delta^{18}O$ and $\delta^{13}C$ values*

The results of stable carbon and oxygen isotope analyses of the Kocabaş travertines are summarized in Table 2 and plotted in Fig. 4. According to result of stable isotopic analyses, Kocabaş travertines has  $\delta^{18}O$  Vienna Pee Dee Belemnite (VPDB) values from -6.4‰ to -10.4‰ and  $\delta^{13}C$  VPDB values from 1.1‰ to 2.6‰ (Table 2). Isotope values have correlated with pollen results in palynological record part (Figs. 8&9).

Variations in  $\delta^{18}O$  of travertine are the result of complex interactions of different environmental factors which are temperature, altitude, latitude, continental, amount, source, seasonal and ice volume effects (Gat, 1996; Rozanski *et al.*, 1993; Clark & Fritz, 1997; Lykoudis *et al.*, 2010; Lachniet, 2009). Largest variations in the isotopic composition of precipitation are related to evaporation and condensation processes of the atmospheric air masses (Gat, 1996). Besides, the mean annual temperature at a given location is positively correlated with the mean  $\delta^{18}O$  value of the local precipitation. A higher mean temperature leads to a higher  $\delta^{18}O$  value in the local precipitation (Gat, 1996).

The  $\delta^{13}C$  of values is mainly result of the relative contribution between carbon extracted from soil-captured or atmospheric carbon dioxide and taht from dissolution of carbonates. This main signature can be seriously altered by several factors such as evaporaiton and degassing. The  $\delta^{13}C$  of values is also related to the plant distribution. For example, warmer and wetter climatic conditions would lead to a higher proportion of C3-plants which are mainly building up of trees and plants growing in the higher and middle latitudes (McDermott, 2004). C4-plants (e.g. grasses, sedges and straw) are specialized to survive in dry and open ecosystems like tropical and temperate grasslands (Clark & Fritz, 1997; Spötl,

2001/2002). During the  $\delta^{13}\text{C}$  curve is not observed significant changing. However,  $\delta^{13}\text{C}$  values are positive part of the scale and resemble values (Fig. 6) and this resemble values could be indicated non-changing plant distribution. However, there is minor decreasing and increasing of the  $\delta^{13}\text{C}$  curve is showed and this minor differentiation is recorded levels which are observed maximum changing of the  $\delta^{18}\text{O}$  curve and travertine with straw fossils.

**Table 2.** Stable isotopic results from Kocabaş quarries.

Sample No	$\delta^{13}\text{C}$ (V-PDB)	$\delta^{18}\text{O}$ (V-PDB)	$\delta^{18}\text{O}$ (V-SMOW)	Sample No	$\delta^{13}\text{C}$ (V-PDB)	$\delta^{18}\text{O}$ (V-PDB)	$\delta^{18}\text{O}$ (V-SMOW)
S4-1K	1.8	-8.9	21.8	S4-31 K	1.6	-8.6	22.1
S4-2K	1.7	-9.7	20.9	S4-32 K	1.7	-8.1	22.5
S4-3 K	1.4	-10.1	20.5	S4-33 K	1.9	-9.3	21.3
S4-4 K	1.3	-9.8	20.9	S4-34 K	2.0	-9.5	21.1
S4-5 K	1.4	-9.4	21.2	S4-35 K	1.8	-8.7	22.0
S4-6K	2.2	-8.7	22.0	S4-36 K	1.5	-8.7	21.9
S4-7 K	1.9	-8.8	21.8	S4-37 K	1.8	-8.0	22.6
S4-8K	1.9	-8.2	22.5	S4-38 K	1.5	-1.5	20.1
S4-9 K	1.8	-7.3	23.4	S4-39 K	1.5	-1.1	20.5
S4-10K	1.9	-7.9	22.8	S4-40 K	1.4	-10.1	20.5
S4-11K	1.7	-7.2	23.5	S4-41 K	1.7	-10.2	20.4
S4-12K	1.9	-8.8	21.8	S4-43 K	1.1	-10.4	20.2
S4-13K	1.6	-7.6	23.1	S4-44 K	1.2	-10.4	20.2
S4-14K	1.3	-7.2	23.5	S4-45 K	2.2	-9.1	21.5
S4-15K	2.2	-8.7	21.9	S3-1 K	1.9	-7.6	23.1
S4-16K	1.9	-8.4	22.2	S3-2K/a	2.0	-9.5	21.1
S4-17K	1.9	-7.9	22.7	S3-2K/b	1.9	-9.2	21.5
S4-18K	1.8	-7.8	22.9	S3-3 K	1.8	-9.1	21.6
S4-19K	1.8	-8.9	21.8	S3-4 K	1.7	-8.1	22.5
S4-20K	1.9	-8.1	22.6	S3-5 K	1.8	-7.2	23.5
S4-21K	1.9	-8.4	22.2	S3-K/a	2.0	-7.4	23.3
S422 K	1.9	-8.1	22.6	S3-6K/b	1.7	-6.4	24.3
S4-23K	1.9	-7.8	22.9	S3-7 K	1.7	-8.4	22.2
S4-24K	1.9	-9.5	21.1	S3-8 K	1.6	-7.1	23.6
S4-25K	1.9	-8.2	22.4	S3-9 K	2.6	-8.6	22.1
S4-26K	2.0	-9.2	21.5	S3-10 K/a	2.6	-8.3	22.4
S4-27K	1.8	-8.1	22.6	S3-10 K/b	2.6	-8.2	22.5
S4-28K	1.8	-8.7	21.9	S3-11 K	2.5	-8.2	22.4
S4-29K	1.5	-8.4	22.2	S3-12 K	2.2	-9.1	21.5
S4-30K	1.5	-8.7	21.9	S3-13 K	2.5	-8.7	21.9

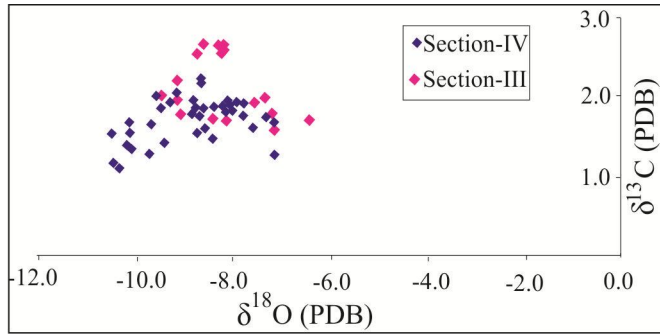


Fig. 5. Stable carbon versus oxygen isotopic cross-plot for Kocabaş travertines (Site-III and Site-IV).

### *Age Determinations*

U/Th age of thirteen dated travertine samples is given in Table 3, together with the different isotopic ratios and absolute ages. Samples obtained from travertine benches from 11 out of 13 samples provide reliable results (Table 3). The U/Th method yielded glacial and late glacial ages (Table 3). The isotopic ratio of  $^{230}\text{Th}/^{232}\text{Th}$  pointed out the degree of sample contamination and the determination of this ratio indicates the reliability of the final results, because the absolute age shows older values when the sample is contaminated with terrigenous content. If travertines ages obtained are  $^{230}\text{Th}/^{232}\text{Th} > 17$  more reliable, on the other hand when  $^{230}\text{Th}/^{232}\text{Th} < 10$  the obtained dates from the sample are too old (Julia & Bischoff, 1991).

Kocabaş shallow lake-type travertine body (Site-II) yielded the oldest ages among the dated samples, showing an age of approx.  $181.26 \pm 7.7$  kyr, even though the  $^{230}\text{Th}/^{232}\text{Th}$  ratios were  $< 17$ . The travertine body (Site-IV) gave the youngest age (approx.  $85.51 \pm 5.8$  kyr). According to the radiometric dating, travertine precipitation started in the Late Pleistocene corresponding to the glacial and last interglacial periods in marine isotopic stage (MIS6 and MIS5).

**Table 3.** U/Th isotopic compositions and radiometric age data of travertine samples from Kocabaş. Samples with significant detrital contamination are related to  $^{232}\text{Th}/^{230}\text{Th} < 10$ . This contamination, in general renders too old nominal date calculated from  $^{230}\text{Th}/^{234}\text{U}$ . Six samples are less purity related to  $^{230}\text{Th}/^{232}\text{Th} < 17$ .

Sample	$^{238}\text{U}$ (ppm)	$^{232}\text{Th}$ (ppm)	$^{234}\text{U}/^{238}\text{U}$	$^{230}\text{Th}/^{234}\text{U}$	$^{230}\text{Th}/^{232}\text{Th}$	Ages (kyr)
S1-10K	0.3533	0.0045	1.2145±0.008	0.6281±0.004	184.559±1.16	<b>103.778±1.4</b>
S1-5K	0.1060	0.018	1.2096±0.009	0.8987±0.007	197.4037±2.1	Age calculated do not converge
S1-1K	0.1372	0.0037	1.2148±0.007	0.8168±0.007	113.821±1.09	<b>169.335±3.8</b>
S2-10K	0.3132	0.0877	1.2119±0.007	0.6578±0.006	8.6968±0.09	<b>104.000±3.9</b>
S2-1K	0.0723	0.0169	1.2120±0.008	0.8522±0.009	13.5088±0.1	<b>181.267±7.7</b>
S3-14K	0.1920	0.0100	1.393±0.01	0.6929±0.01	54.2065±0.5	<b>118.3170±3</b>
S3-12K (b)	0.2157	0.0026	1.2184±0.03	0.7058±0.01	217.4143±4	<b>125.9506±3</b>
S4-39K	0.3764	0.2103	1.4626±0.01	0.6097±0.009	4.8774±0.08	<b>85.512±5.8</b>
S4-41K	0.3450	0.0058	1.2473±0.009	0.6440±0.008	7.3117±0.1	<b>99.865±4.5</b>
S4-38K	0.4051	0.1835	1.2585±0.007	0.6764±0.008	5.7433±0.08	<b>106.217±5.9</b>
S4-32K	0.1282	0.0294	1.2400±0.01	0.7377±0.01	12.1999±0.2	<b>131.493±4.8</b>
S4-20K	0.1461	0.0276	1.2263±0.01	1.0696±0.01	21.2362±0.1	Age calculated do not converge
S4-15K	0.1109	0.0182	1.2263±0.009	0.7474±0.01	17,0234±0.2	<b>139,9060±4</b>

### Palynological Records

Palynological research has been examined all sections in site by site, separately and given belloved in detailed.

#### *Site I*

This section starts the 169.335±3.8 BP (sample S1-1K) and it ends 103.778±1.4 BP (samples SI-10K) relating to dating results and also this time interval represents between MIS 6 and MIS 5c stages (Fig. 6; Table 3). The pollen diagram of section-I from Site-I is shown in Fig 6.

The palynological samples are only collected from the paleosol sediments (L8) in the lower part of the section of Site I. It is interesting to note that palynoflora of this site is characterized by high abundance of the nonarboreal species. Compositae-Tubulifloreae and Ligulifloreae types of these species are recorded high percentage in the palynospectra and also other grassland species (Geraniaceae, *Artemisia*, Chenopodiaceae and Apiaceae) accompanied with these types. *Quercus* evergreen type is abundantly observed and *Pinus*, *Abies*, *Salix*, *Castanea*, *Fraxinus*, *Polygonum*, *Isoetes*, Oleaceae of arboreal species was recorded less abundant (Fig. 6c).

According to the palynoflora, open vegetation area widespread during the warm phase of MIS 6 stage. Abundance of the NAP percentage and xerophytic plant (Oleaceae and *Quercus* evergreen type) indicate drought and support the last warming in the MIS 6 (Fig. 6d). Besides, presence of the *Isoetes* indicates the summer dryness and wet winter half year. Paleosol deposition is not coincidence in the last warming phase of the MIS 6 stage because this warming phase in this stage could be caused decreasing of the water level of the lake and dry condition in the land (Fig. 6c). Besides, after than the MIS 6 phase in the section I, sedimentary facies are represented by the L1, L2 and L3 lithotypes which indicate the increasing water level in lake during the MIS 5e-d stages (Fig. 6).

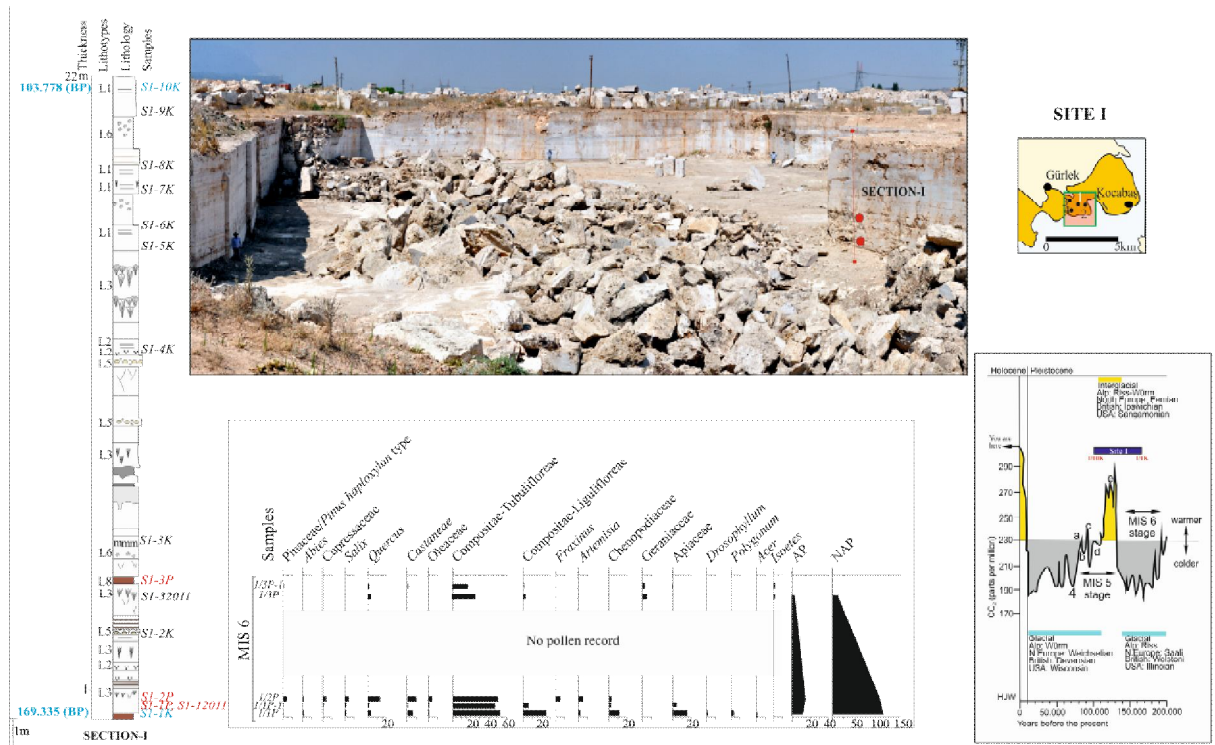


**Fig. 6.** a,b) Measured stratigraphic section of the Site-I and study area, c) pollen diagram of the Site I in the Kocabaş area, and d) isotopic stages of the Late Pleistocene and Holocene.

### Site II

Based on the  $^{230}\text{Th}/^{234}\text{U}$  isotope ration, deposition of the Site II starts the  $181.267 \pm 7.7$  kyr (MIS 6) (sample S2-1K) and it ends  $104.000 \pm 3.9$  BP (MIS 5d) (samples S2-10K) (Fig.7; Table 3). Palynological samples are collected from the three paleosol level (L8) of the stratigraphic Section-II. The pollen diagram of this section from Site-II is shown in Fig.7. Three palynological contents are defined and first palynoflora obtained from the lower part of the section such as pollens (*Pinaceae-Pinus*, *Compositae-Tubuliflorea* and *Fraxinus*) are less abundantly recorded. The second palynoflora is defined from the middle part of the section and it is included rich and a few various pollens. The most important plant belongs to *Pinaceae* (*Pinus* and *Abies*) and this plant is defined more abundantly in the palynospectra. Grassland species (*Compositae-Tubuliflore* and *Chenopodiaceae*) are rare. Other pollens (*Carpinus*, *Salix*, *Quercus*, *Oleaceae*, *Pterocarya*) are accompanied with *Pinaceae*.



Abundance of the Pinaceae could be interpreted high topography near the deposition area and/or high pollen transport. However, less abundantly observing of Pinaceae in other palynospectras and presence of the *Corylus* in the second palynoflora could be indicated the effective palaeoclimatic condition.

Based on palynological data cooling of the end of the MIS 6 stage could be caused the abundance of Pinaceae during the travertine deposition in this area. The last palynoflora is recorded upper part of the section II and it is characterized by the decreasing of the Pinaceae, frequent and low percentage of the nonarboreal pollens (Compositae-Tubuliflore, Centaureae and Poaceae). This floral changing could be indicated the palaeoclimatic changing although there are not significant palaeotopographing changing. Palaeoclimatic event from the MIS 6 to MIS 5e could be explained this floral changing and observing of nonarboreal pollens in the terrestrial area could be associated with the warm climatic condition in the MIS 5e. Presence of the L3 lithotypes indicates the suitable condition for the C4-plant during the warm phase of the MIS 5e stage. The L5, L6 and L1 lithotypes are observed end of the stratigraphic section (MIS 5d; 104.000 BP) and this could be showed the increasing the water level in the lake. This environmental change in the lake could be related to cooling phase in the MIS 5d stage as the end of the Section-I in the Site-I.

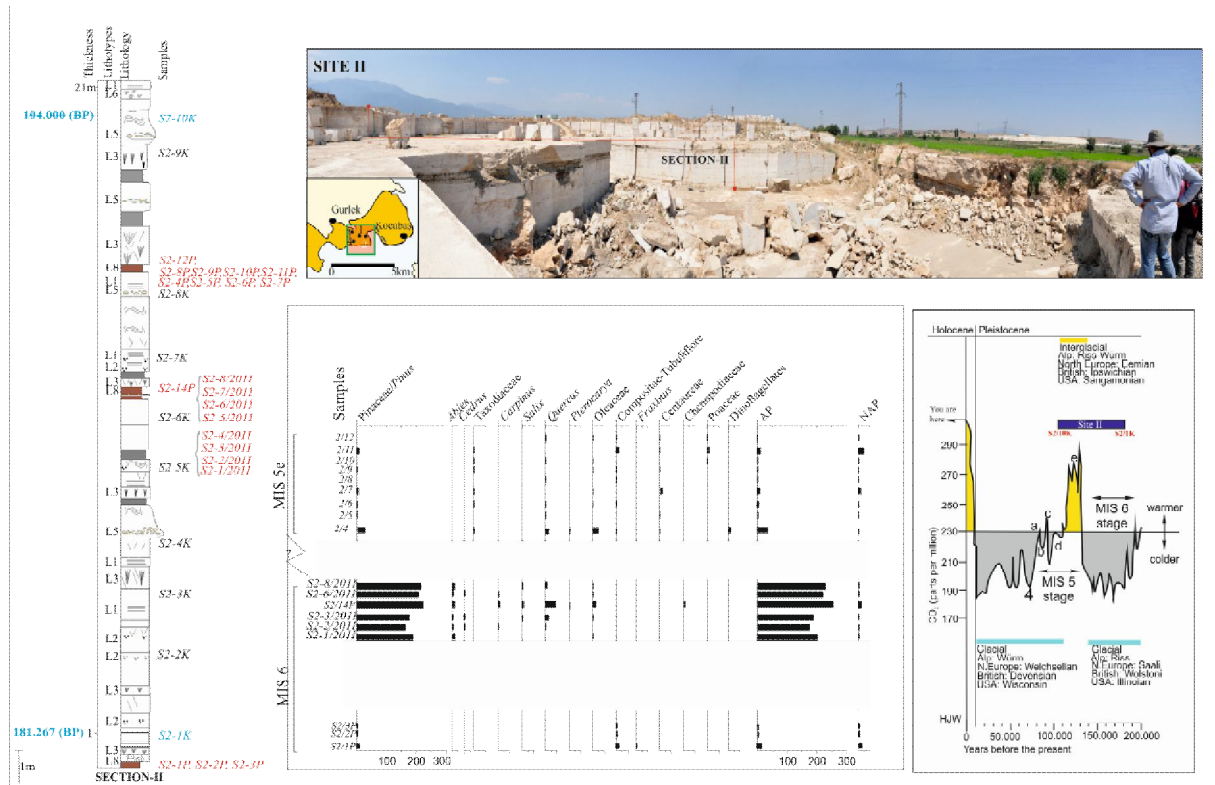


**Fig. 7.** a) Measured stratigraphic section of the Site-II and study area b) pollen diagram of the Site-I in the Kocabaş area, and c) isotopic stages of the Late Pleistocene and Holocene.

### Site -III

According to the two  $^{230}\text{Th}/^{234}\text{U}$  isotope ratios (S3-12K sample:  $125.9506 \pm 3\text{kyr}$  and S3-14K sample:  $118.317 \pm 3\text{kyr}$ ) most of sediments in the Site-III is deposited during the MIS 5 stage (Fig. 8). Palynological samples in this site are collected from the claystones in lower part of the stratigraphic Section-III and these samples are not suitable for the palynological study. For this reason, this site tried to explain by stable isotopic values. (Fig 8).

According to stable carbon and oxygen isotope measurements from the travertine precipitations in the Site- III, the measured isotope compositions vary within wide ranges: the  $\delta^{13}\text{C}$  values range between  $+2.6\text{‰}$  and  $+1.6\text{‰}$  (V-PDB) and the  $\delta^{18}\text{O}$  values vary between  $+21.1\text{‰}$  and  $+24.3\text{‰}$  (V-SMOW) (Table 2) . There are three distinctly decreasing of the  $\delta^{18}\text{O}$  values which indicated the cooling of the palaeoclimate (Fig. 8). Travertines samples

which are obtained decrease  $\delta^{18}\text{O}$  values belongs the L1 and L2 lithotypes. According to this evident, palaeoclimate is cooling while laminar travertines are depositing. Warming period which are characterized by the increasing of the  $\delta^{18}\text{O}$  values are represented by the L3 lithotype and also faunal and floras composition in this facies widespread. This rich composition of plant and gastropod could be related to the shallowing of the lake water because of the palaeoclimatic warming.

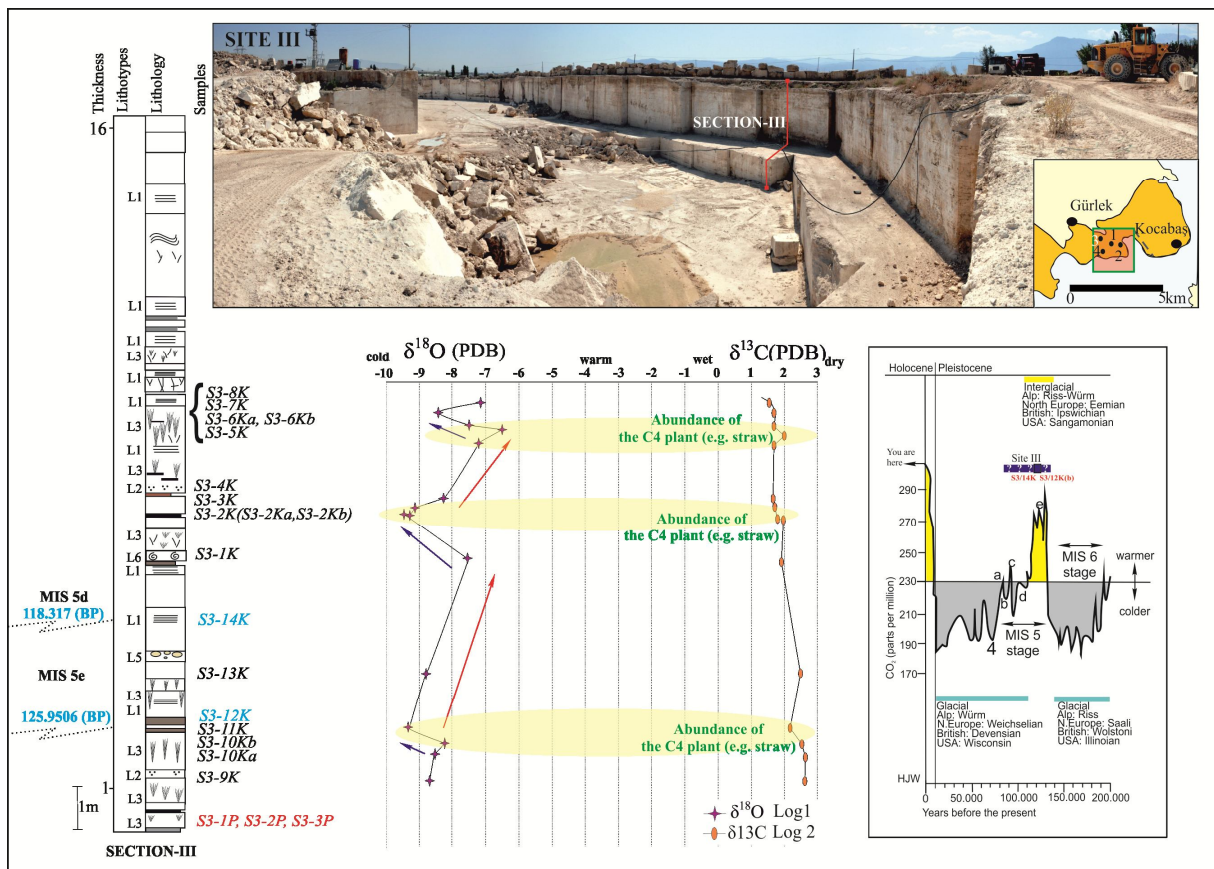


**Fig. 8.** a) Measured stratigraphic section of the Site III and study area, b) Oxygen and carbon isotope curves, and c) isotopic stages of the Late Pleistocene and Holocene.

#### *Site IV*

Based on the  $^{230}\text{Th}/^{234}\text{U}$  isotope ratios (S4-15K sample:  $139.9060 \pm 4\text{kyr}$  and S4-39K sample:  $85.512 \pm 5.8\text{kyr}$ ), sediments in the Site-IV is deposited from the MIS6 to MIS4 stage (Fig.9). Eighteen claystones samples of the paleosol levels are collected for the palynological study. These are located upper part of the section-IV. Besides, level with leaf fossils which are could be belonged Fagaceae-*Quercus* of the C3-plant are observed in lower part of the section. Additionally gastropods and crab fossils are collected from the detritus of the L6 lithotype and paleosol level (Fig. 9).

The first palynological record of the  $106.217 \pm 5.3$  (kyr) is obtained twelve claystone samples of the paleosol sediments. Palynoflora of this time is represented by abundance of the C3-plants and it consists of more abundant Pinaceae (*Pinus* and *Abies*), *Quercus* and Oleaceae. C4-plants (Ericaceae, Compositae-Tubuliflorea type, *Phillyrea* and Chenopodiaceae) are recorded less abundant in the palynospectra.

Abundance of the *Pinus* and *Abies* species could be indicated the cold climatic condition and this climatic interpretation in end of the MIS 5d of the Site IV coherents with global climatic data (Fig. 9). Besides, the  $\delta^{13}\text{C}$  of value from S4-15K to S4-43K sample decreases. This decline could be showed the wet climatic condition during deposition between these samples and this humidity explains abundance of the Pinaceae. The second palynoflora is defined end of the stratigraphic section of Site IV and it is characterized by the C4-plants which are only represented by the grassland species (e.g. Compositae-Tubuliflorea type, Chenopodiaceae, Poaceae). Decreasing of the  $\delta^{13}\text{C}$  of value could be related to abundance of the C4-plants.

There are five distinct changes of the  $\delta^{18}\text{O}$  values during the stratigraphic section-IV and the first one is recorded from the early phase of the MIS 6 stage in the section-IV. In this phase, decreasing of the  $\delta^{18}\text{O}$  values are observed and this indicates the cooling in the

palaeoclimate. The second change is showed upper part of the MIS 6 stage which is represented by the increasing of the  $\delta^{18}\text{O}$  values. Based on the  $\delta^{18}\text{O}$  result in this part, warming in the palaeoclimate is recorded. Throughout the MIS 6 and MIS 5 boundary, the  $\delta^{18}\text{O}$  values change frequently and the  $\delta^{18}\text{O}$  values are generally high during this boundary. Sample of the MIS 5e and MIS 5d phased is not collected because the lithology is not suitable for the isotopic study. These phases are represented by the L6 sedimentary lithotype. Though there are not recorded palaeoclimatic changing in the MIS 5e, cooling are observed from the MIS 5e to MIS 5d based on the  $\delta^{18}\text{O}$  values. This cooling in the study area could be matched the global glacial in the MIS 5d. Sedimentary deposition during the MIS 5b stage is little. MIS 5c and MIS 5a phases are characterized by the increasing of the  $\delta^{18}\text{O}$  values and this increasing could be correspond to the warming phase in the MIS 5c and a. MIS 4 stage is recorded upper part of the stratigraphic section IV and there are decreasing and increasing of the  $\delta^{18}\text{O}$  values during the MIS 4 phase, respectively. This changing could be explained the fluctuations in the palaeoclimate during the MIS 4 phase.

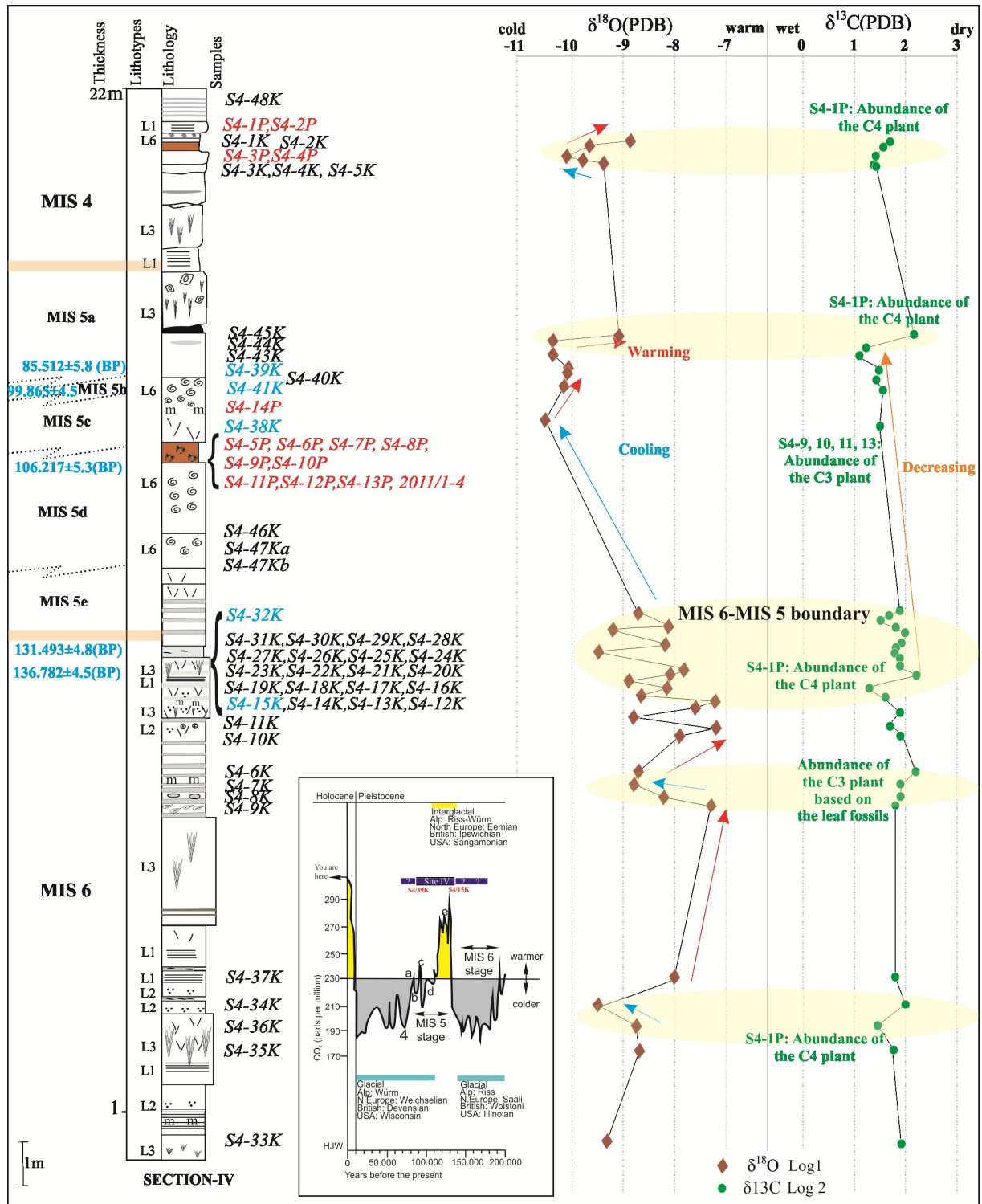


**Fig. 9.** a) Measured stratigraphic section of the Site IV and study area, B) Oxygen and carbon isotope curves, and c) isotopic stages of the Late Pleistocene and Holocene.

## DISCUSSIONS

### *Palaeoenvironmental reconstruction: depositional model and comparison to other lacustrine travertines*

The sedimentological analysis of the facies indicates that the Kocabaş travertines have been deposited in shallow lake fill or pool environment (Fig. 10). When this kind of travertine precipitation compared to other lacustrine travertine outcrops considering lithotypes, facies, fauna, flora, erosional surface, lateral extension, thickness, age range, depositional environment and processes, has some similarities with each other (Table 4). Lithotypes are mostly composed of laminated, coated bubble, reeds, paper-thin raft, intraclasts, gastropods and paleosols although crystalline crust, shrub, pisoid have been also found as well (etc. Bagno di Tivoli, Rapolano Terme and Ballık) (Chafetz & Folk, 1984; Faccenna *et al.*, 2008; Guo & Riding, 1998; Brogi & Capezzuoli, 2009; Özkul *et al.*, 2002). Furthermore, Rapolano Terme has showed same facies with Kocabaş tavertines such as marsh pool and shrub flat facies but Bagni di Tivoli has also terrace-mound and sloping mound facies (Guo & Riding, 1998; Brogi & Capezzuoli, 2009). Fauna and flora in the study area have showed that some variations among them, on the other hand erosional surface such as paleosol and karstic features are indicative structures in the field (Table 4). Thickness of the travertine benches is more or less close to each other however age results obtained merely two of them has been observed some differences. Bagni di Tivoli travertines have begun to precipitate earlier than Kocabaş travertines (Table 4).

Table 4. Comparison of the Kocabaş travertines with other shallow lake-fill type travertine deposits.

	<b>Bagni Di Tivoli</b> (Chafetz & Folk, 1984; Faccenna <i>et al.</i> , 2008)	<b>Rapolano Terme</b> (Guo & Riding, 1998; Brogi & Capezuoli, 2009)	<b>Balıkk</b> (Özkul <i>et al.</i> , 2002)	<b>Kocabaş travertines</b> (this study)
<b>Lithotype</b>	Dominantly bacterial shrubs, layers of intraclasts, pockets of pisoids	crystalline crust, shrub, pisoid, paper-thin raft, coated bubble, reed, lithoclast-breccia, paleosol	Crystalline crust, shrub, pisolith, paper-thin raft, coated gas bubble, reed, lithoclast, pebbly travertine, paleosol	Laminated, coated bubble, reeds, paper-thin raft, intraclasts, gastropods, paleosol
<b>Facies</b>	Shrub facies, terrace-mound facies, sloping-mound facies	Shrub flat facies, marsh-pool Facies	Pisolith, paper-thin rafts, coated gas bubble, reed, lithoclast, pebbly and paleosols	Shrub flat facies, Marsh pool facies
<b>Fauna</b>	Plethora (tiny oval bodies, about 0.5x1.0µm and 2), blue-green algae, red and green algae, fungi	Ostracodes, gastropods are locally common	Diatome, gastropods, bacterial filaments, irregular radial pisoliths (bacterially mediated)	Gastropods, crap fragments,
<b>Flora</b>	Leaves, woody plants, shrubs, branches (stem or trunk)	Reeds	Reed, shrubs,	Pollens ( <i>Abies</i> , <i>Pinus</i> , <i>Quercus</i> , Compositae-Tubulifloreae)
<b>Erosion surface</b>	Five main erosional surfaces; paleosols, conglomerates and karstic features	Clay-silt paleosols	Solution cavities, microkarstic features	Palaeosols, karstic features
<b>Lateral extension</b>	200-300 m	Tens to hundreds of meters	Hundreds of meters	A few hundred meters
<b>Thickness</b>	85 m	40 m	65 m	60 m
<b>Age range</b>	30-115 ka	-----	-----	85-181 ka
<b>Depositional environment</b>	Shallow lake	Flats and hollows in areas of relatively low topography	Depression depositional (shrub flat and marsh-pool subenvironments)	Depression depositional system like stagnant/low energy lake environment.
<b>Depositional process</b>	Very shallow lake-fill deposits and terrigenous-rich layers are flood deposits transported from surrounding countryside into the lakes by severe storms	Precipitation from fast flowing spring water, low angle slopes, fine lithoclast shows widespread pedogenic effects.	Terrigenous materials are interpreted as floodings and ephemeral streams are associated with shrub.	Terrigenous materials can be explained by floodings, and hill-wash breccias are lower slope deposits into shallow depressions.



Figure 10 presents a sedimentary facies model based mainly on Late Pleistocene Kocabaş travertine occurrences, which at present are not actively forming travertine or tufa precipitation in this region. This model also shows palaeoclimatic and palaeovegetational evolution from marine isotopic stage MIS 6 to 4. Basically, this model depicts the associations of facies that result from initial tectonic extensional activity and faulted. Thermal water upcoming to the surface which is rich in dissolved  $\text{CaCO}_3$  commenced to precipitate on Neogene clastics such as sandstone, claystone and marl, and later stage of carbonate sedimentation in laterally related pool subenvironment.

According to Figure 10-A travertine precipitation commenced between 170 to 140kyr (glacial period) in a lacustrine environment and palaeovegetation mostly composed of straws and some herbs and shrubs in locally. It has clearly seen Site-I, Site-II, Site-III and Site-IV in this block diagram (Fig.10-A).

During the last interglacial period (140-80kyr) travertine precipitation continued and Figure10-B model obviously correspond to stagnant pool environment. Flat pool, Shrub flat and Marsh pool facies are dominant in this environment. The scheme also shows abundance of gastropods, ostracods and crabs related to the palaeoclimatical warming and most probably it can be assumed that existed appropriate conditions for livings.

The last model corresponds to glacial period marine isotopic stage 4 (80-70kyr) and travertine precipitation progressively has continued to the southwest (Fig.10-C). Travertine precipitation has stopped in Site-I and Site-II whereas Site-III and Site-IV has still continued. This movement can be interpreted to have been developed in a relative depression controlled by local tectonics.

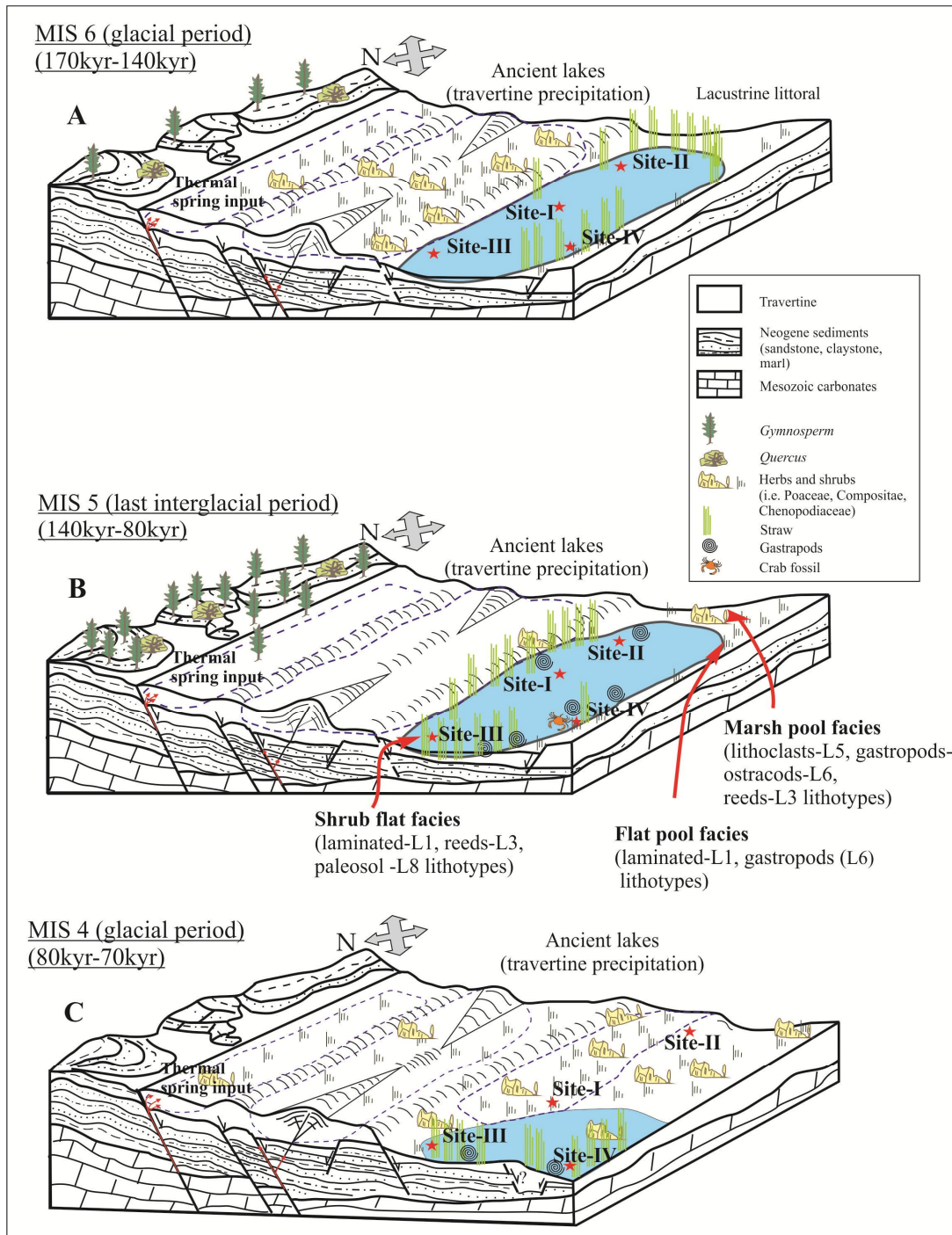


Fig. 10. Schematic block diagrams illustrating the paleoenvironmental evolution of the Kocabaş (Gürlek) area during the Pleistocene. (A) The travertine precipitation in the lacustrine environment (included Site-I and Site-II sections) may have continued until MIS 5 (inter glacial period) regarding to U/Th data and (B) by the way, this travertine precipitation were deposited on the flat pool, shrub flat and marsh pool facies. (C) At the same time, travertine depositional pool may have progressed to the south and continued until MIS 4 (glacial period).

*Palaeoclimatic implications: pollen records, stable isotopic signals and dating*

Travertine deposition is correlated with warm and cold climatic conditions (Pentecost, 1995; Frank *et al.*, 2000 ; Horvatincic *et al.*, 2000). The Kocabaş travertines precipitated in depressional depositinal system seem to have distinctive climatic significance because the obtained precise ages fall within the warm and cold periods evidenced in the marine palaeoclimatic  $\delta^{18}\text{O}$  record as shown in Fig. 11 and also given oxygen and carbon isotope records from Site-III and Site-IV. Travertine from Kocabaş can be attributed within isotopic stage from 6 to 4 (Fig.11).

Pollen stratigraphy shows various vegetational phases distinguishable on the basis of the AP-NAP (arboreal pollen and non-arboreal pollen) diagram. In the time interval from 181kyr to 81kyr following phases haven been recognized Site by Site.

Palynofloras of the MIS 6 and MIS 5d, 5a period are identified and according to our results Palynoflora of the MIS 6 are recorded from the lower part of the section of Site I (169kyr and Site II (older than 181kyr) (Figs 6,7&11). Palynofloras of the Site-I and Site-II are represented by the NAP taxa (Compositae-Tubulifloreae type, Chenopodiaceae, Geraniaceae and Apiaceae) and also Fagaceae-*Quercus*-evergreen type, Castaneae, Oleaceae, *Pinus haploxylon* type, *Isoetes* and *Polygonum* accompanies to the NAP taxa. During the 130 kyr and 153 kyr time interval, warm phase in the MIS 6 is recorded in the middle part of the MIS 6 period based on the oxygen and carbon isotope analysis. Palynofloras of the Site-I for the 169 kyr and Site-II for the 181 kyr are characterized by abundances of herbaceous plants and this evidence could be indicated presence of the warm phase in the MIS 6 period.

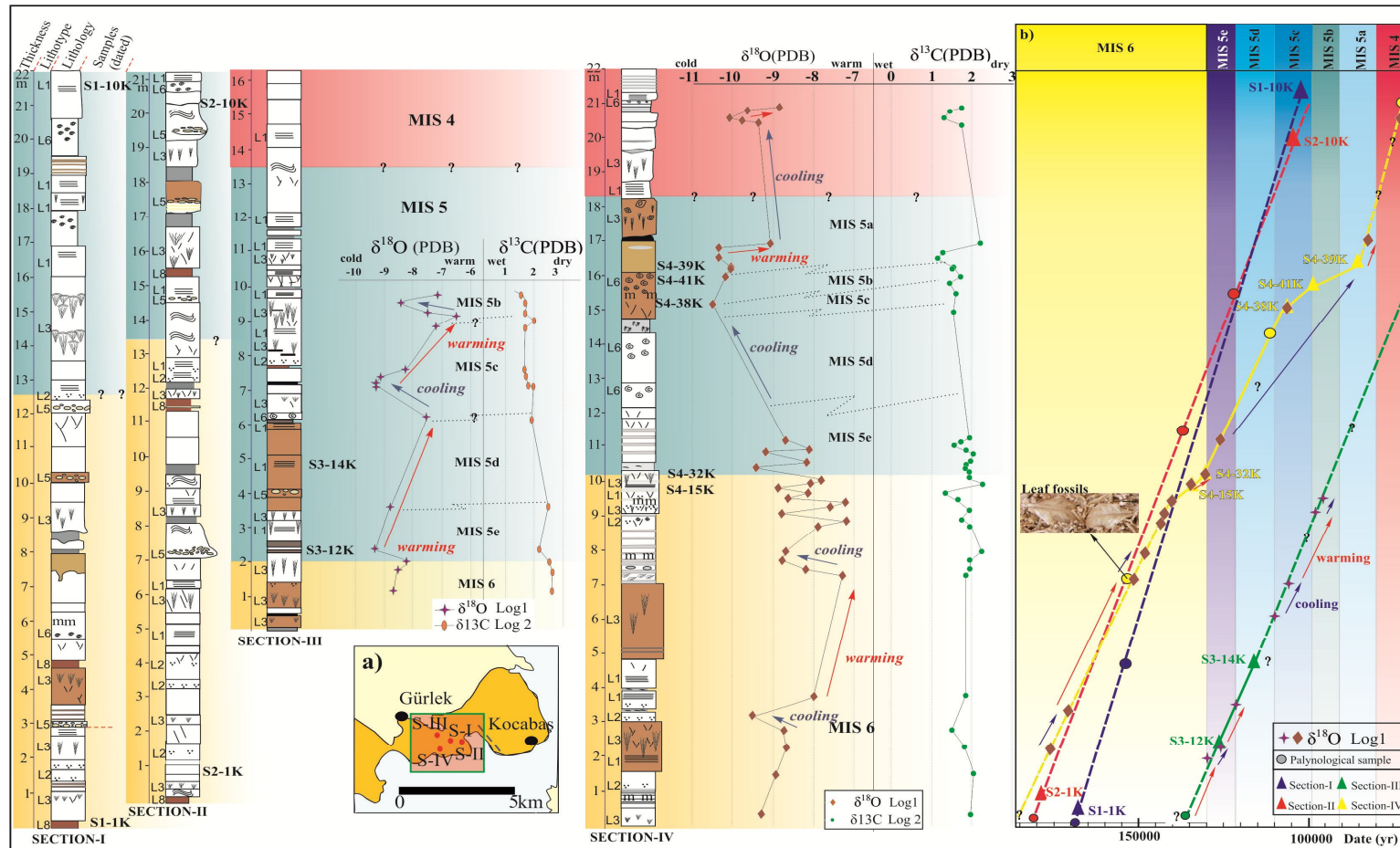


Fig. 11. Illustrated correlation chart of the facies, depositional time (U/Th dating) and stable isotopic curves of the study sites in the Kocabaş area. a) showing the map of the study area and measured stratigraphic sections b) travertine precipitated time from MIS 6 to MIS 4 and illustrated stable isotopic ( $\delta^{18}\text{O}$  and  $\delta^{13}\text{C}$ ) and palynological sample points.

MIS 5d period is recorded from upper part of the stratigraphic section of the Site-II (older than the 104 ka) and Site-IV (older than the 106 ka). This period in both sites, abundance of *Abies*, *Pinus-haploxylon* and *diploxylon* types, Oleaceae, Fagaceae-*Quercus* evergreen type and scarce of grassland species (*Centaurea*, Chenopodiaceae, Poaceae and Compositae), Oleaceae, *Isoetes*, *Cedrus*, *Salix*, *Carpinus*, *Pterocarya* are represented. Palaeoclimate indicates fluctuations during the MIS 5e (Eemian time) and the first cool phase in the MIS 5 (between 90ka and 110 ka) is observed in the MIS 5d (Figs. 5,8& 10). Abundance of the gymnosperm pollen species in our palynospectra of the Site-II and Site-IV could be interpreted cool climatic condition in the MIS 5d period and this palaeoclimatic conditions coherent with the palaeoclimatic trend in MIS 5d period of the world.

In our study, MIS 5a period is only recorded from upper part of the Site IV (~80 ka) and this period represented by the herbaceous species (e.g. Compositae-Tubuliflorea and Ligulifloreae types, Chenopodiaceae and Poaceae). The MIS 5a period is in the warm phase of glacial period and plant distribution in the Kocabaş area during the MIS 5a time could be affected by this warming phase (Fig.11).

In conclusion, the formation of the Kocabaş travertines provides information on the warm and cold periods recorded in the continental environment. Sections I, II and IV represent thick precipitations during MIS 6 period (Fig.10). Deposition of the MIS 5 phase is observed all sections and MIS 4 are only recorded in the Sections III and IV (Figs.6& 8). The  $\delta^{18}\text{O}$  values between the MIS 6 and MIS 4 phases are changeable and this difference could be related to the palaeoclimatic and orographic changing. Besides  $\delta^{13}\text{C}$  indicates the changing based on the plant distribution and these plants could be grown in the lake margin. Tectonic and palaeoclimatic effects have a important role of lake level changes and for that reasons, travertine deposition in the section I and II could be finished in the MIS 4 phase (Figs. 7, 8&11). Palaeoclimatic condition of the end of the MIS 6, MIS 5e and MIS 5d phases could be

correlated based on the sedimentary facies and  $\delta^{18}\text{O}$  values. Ending of the MIS 6 stage is observed the fluctuations in the section IV, however this stage is regularly passed to the MIS 5 stage in the section III. The MIS 5e phase starts the warming and continues the cooling in both sections. The MIS 6 stage is generally represented by the C4-plants in section I and II (grassland species and straws). Based on the palynological date in the section II and IV, lower part of the MIS 5 (MIS 5e and d) stage represented by the C3-plants (e.g. Pinaceae, *Quercus*, Oleaceae, *Abies*). Besides, less abundance of the C4-plants are also recorded in this section. Passing to MIS 4 stage could be evaluated by the theoretical.

## CONCLUSIONS

Conclusions inferred in the study are as follows:

1. Kocabaş travertines have been studied in four juxtaposed outcrops such as Site-I, Site-II, Site-III and Site-IV. Travertine precipitations at Kocabaş have been separated into seven lithotypes and one erosional horizon in the field scale. These are: Laminated, Coated bubble, Reed, Paper-thin raft, Intraclasts, Micritic travertine with gastropods, extra formational pebbles and palaeosol layer. Geochemical analysis, dating, palynological analysis and petrographical investigations have been made on the travertine and detritic samples taken from all outcrops.
2. The travertines in the study area are mainly precipitated on the Depressional Depositional System which is composed of flat pool, shrub flat and marsh-pool facies.
3. According to the stable isotope analysis of the travertine samples, the values of  $\delta^{13}\text{C}$  and  $\delta^{18}\text{O}$  changes between -6.4‰ to -10.4‰ and 1.1‰ to 2.6‰, respectively.
4. Palynological analysis has been done site by site on the samples which are only collected from the paleosol sediments. Site-I, Site-II and Site-IV are According to results, palynoflora of Site-I is characterized by high abundance of the nonarboreal species. Compositae-

Tubulifloreae and Ligulifloreae types of these species are recorded high percentage in the palynospectra and also other grassland species. Site-II is characterized the most important plant belongs to Pinaceae (*Pinus* and *Abies*) and this plant is defined more abundantly in the palynospectra. Grassland species (Compositae-Tubuliflore and Chenopodiaceae) are rare in this site. Furthermore, other pollens (*Carpinus*, *Salix*, *Quercus*, Oleaceae, *Pterocarya*) are accompanied with Pinaceae. Site-III is very poor for palynological study whereas Site-IV is mostly represented leaf fossils which are could be belonged Fagaceae-*Quercus* and some crap fragments as well as pollens. Site-IV also consists of more abundant Pinaceae (*Pinus* and *Abies*), *Quercus* and Oleaceae and at the same time, Ericaceae, Compositae-Tubuliflorea type, *Phillyrea* and Chenopodiaceae are recorded less abundant in the palynospectra.

5. Travertine deposition at Kocabaş area occurred during late Pleistocene time (i.e., between 180-80kyr) and they have formed in a series of climatic changes during glacial and interglacial intervals. They can be referred to warm marine oxygen isotopic stage 5 and cold marine oxygen isotopic stages 6 and 4.

6. The sedimentological, palynological analyses indicate that the Kocabaş travertines have been deposited in shallow lake fill or pool environment. Travertine precipitation commenced in a lacustrine environment during glacial period MIS 6. Thick travertine deposits can be observed in last interglacial period MIS 5. Travertine precipitation has ended in Site-I and Site-II whereas Site-III and Site-IV has still continued to accumulate. This is indicated by the fact that, local tectonic activity has a important role of this movement.

## **ACKNOWLEDGEMENTS**

This work was supported financially by project 2010BSP005 of Scientific Research Unit at Pamukkale University.